Semnan University

Journal of Heat and Mass Transfer Research

Journal homepage: http://jhmtr.semnan.ac.ir

Heat Transfer Enhancement in a Spiral Plate Heat Exchanger Model Using Continuous Rods

Soheil Nasrollahzadeh Sabet, Rahim Hassanzadeh *

Faculty of Mechanical Engineering, Urmia University of Technology, Urmia, Iran.

PAPER INFO

Paper history:
Received: 2019-09-24
Revised: 2020-02-23
Accepted: 2020-02-13

Keywords:
Spiral plate heat exchanger;
Continuous vortex generators;
Heat transfer enhancement;
Unsteady flow.

ABSTRACT

In this study, an innovative and simple method to increase the rate of heat transfer in a spiral plate heat exchanger model has been presented. For this purpose, several circular cross-section rods, as continuous vortex generators, were inserted within the spiral plate heat exchanger in the cross-stream plane. The vortex generators were located at various azimuth angles of α=30°, 60°, 90°, and 120° with non-dimensional diameters of d/H=0.3, 0.4, and 0.5. Computations were carried out numerically by means of the finite volume approach under different Dean Numbers (De) ranging from 500 to 1500 in the laminar regime. The flow physics within the advanced spiral heat exchanger model has been discussed using several velocity and temperature contours. It was found that by inserting the continuous vortex generators in the cross-stream plane of a spiral plate heat exchanger, an unsteady flow developed within the channel. The rate of unsteadiness was directly proportional to d/H and De but inversely related to the azimuth angle. The maximum heat transfer enhancement with respect to the conventional spiral plate heat exchanger (without continuous vortex generators) was found to be 341% for α=30°, d/H=0.5, and De=1500. Additionally, values of pressure drop penalty and thermal-hydraulic performance were determined accordingly.

DOI: 10.22075/JHMTR.2020.18783.1251

1. Introduction

Spiral plate heat exchangers are widely used in various industries due to their advantages such as their simple structure, high heat transfer efficiency, low maintenance costs, smaller occupied area, and etc. These kinds of heat exchangers are made by rolling long metallic sheets in two different passages. In this structure, both hot and cold fluids move in two separate spiral passages which have been sealed to avoid any fluid intermixing. Moving the fluid within a spiral passage is under the influence of centrifugal forces and therefore, the flow behavior is different from that of a straight passage. Generally, spiral heat exchangers have two structures, namely, spiral tube heat exchanger or shell and coil heat exchanger or spiral plate heat exchanger. There are many different papers regarding the spiral tube heat exchangers, but the spiral plate heat exchanger has not been investigated widely. Saeidi et al. [1] conducted a study on a novel spiral coil as a ground heat exchanger to augment the thermal performance of a heat pump and found a 31% improvement for their presented model. In addition, Bahiraei and Ahmadi [2] examined the water-alumina nanofluids in a spiral plate heat exchanger under several Reynolds numbers in a range from 4000 to 11000 and nanoparticle volume concentrations varying from 0 to 5%. They obtained a 134.4% enhancement of the convective heat transfer coefficient. Zhao et al. [3] investigated the influence of the spiral pitch of a ground source spiral tube heat exchanger and concluded that a spiral tube heat exchanger with a small pitch had higher energy efficiency in comparison to larger pitches. Li et al. [4] examined a horizontal spiral tube heat exchanger under groundwater advection and found a large influence of the groundwater on the heat exchanger performance. Furthermore, Dehghan [5] examined different arrangements of spiral tube heat exchangers used as ground source heat exchangers and concluded that among the cases under consideration, configurations made by nine spiral heat exchangers were preferable. In other research, fluid-thermal-structural analysis of a spiral wound heat

* *Corresponding Author: Rahim Hassanzadeh, Faculty of Mechanical Engineering, Urmia University of Technology, Urmia, Iran.*
Email: r.hassanzadeh@uut.ac.ir

exchanger was studied by Wang et al. [6] under various parameters such as winding angles, wall thicknesses, tube pitches, and outer diameters of tubes using several inlet velocities varying from 0.5 to 2.5 m/s. They discussed the shell side flow characteristics as a function of the aforementioned parameters and presented several results. For example, by increasing the winding angle, the heat transfer coefficient increased and subsequently decreased. Abdel-Aziz and Sedahmed [7] investigated the natural convective heat and mass transfer in a horizontal spiral tube heat exchanger. They considered several variables such as tube diameter, tube pitch, and physical properties of the working fluid and presented a correlation for the Sherwood number (Sh) based on the obtained data. Sharqawy et al. [8] studied the effect of flow configuration on the performance of a spiral wound heat exchanger for Re=9000-1000 and Re=500-6000 for tube and shell side flows, respectively. It was found that the mixed axial-radial flow configuration provided the maximum heat transfer and pressure drop followed by axial and radial flow configurations. Saedi Ardahaie et al. [9] proposed a novel flat spiral tube heat exchanger for the purpose of energy storage in a solar thermal system. They considered several parameters and various configurations in their study and concluded that the vertical configuration was more capable of storing energy in a specified duration of maximum solar radiation. Mohamad Gholy Nejad et al. [10] investigated the turbulent flow of SiO_2 and Al_2O_3 nanofluids with water as the base fluid in a helical heat exchanger for Re=11600-28120. They compared their results with available experimental data and found maximum errors of 6.56% and 0.27% for friction factor and the Nusselt number, respectively.

To date, several passive methods have been introduced to enhance the heat transfer rate in various types of heat exchangers. Among these passive methods, the use of various vortex generators is more attractive and numerous studies have been published in this regard. For instance, da Silva et al. [11] applied longitudinal vortex generators within a flat plate solar water heater to enhance the heat transfer rate at Re=300, 600, and 900 and attack angles of 15°, 30°, and 45°. They found the best ratio between the heat transfer and pressure drop penalty for the delta-winglet vortex generator at an attack angle of 30°. Effect of the longitudinal vortex generator on heat transfer enhancement of a circular tube was studied by Wang et al. [12]. They considered several parameters such as the spacing length, central angle, and slice height and concluded that the heat transfer and flow resistance increased with the increase of the central angle and slice height and with the decrease of the spacing length. In addition, application of delta-winglet vortex generators in panel radiators was investigated by Garelli et al. [13]. They found a 12% improvement in overall heat transfer. Yang et al. [14] used a wedge-shaped vortex generator in a dimple channel for a constant Reynolds number of 2800. In comparison to the dimple channel without the vortex generator, they obtained an increase of 30% in the goodness factor at a width ratio of 0.4411f between the channel and vortex generator. In another study by Ke et al. [15], they implemented the longitudinal vortex generators in a rectangular channel under Re<2200. They compared several scenarios for arranging the vortex generators such as the common-flow-down, common-flow-up, and mixed configurations. In another work, Jiansheng et al. [16] studied the heat and fluid flow in a rectangular channel in the presence of several miniature cuboid vortex generators for Re=3745 and reported 5.17% and 8.15% improvements for the Nusselt number and thermal-hydraulic performance, respectively. Inclined projected winglet pair vortex generators with protrusions in a rectangular channel were suggested by Oneissi et al. [17] to enhance the rate of the heat transfer for Re=4600. It was demonstrated that inclined projected winglet pair vortex generators with protrusions enhanced the rate of heat transfer 7.1% more than the delta winglet type vortex generators. Samadifar and Toghraie [18] applied a new type of vortex generator in a plate-fin heat exchanger. They identified the best angle of attack for vortex generator installation as 45°. Gallegos and Sharma [19] studied the heat transfer performance of flag vortex generators in rectangular channels for $4\times10^3<Re<5\times10^3$. It was found that using the flag type vortex generators, the Nusselt number increased to 1.34-1.62 with respect to the conventional channel without vortex generators. Li et al. [20] examined the longitudinal vortex generators in a parallel and finless heat exchanger. It was illustrated that by incorporating the double triangle vortex generator, 92.3% heat transfer enhancement was obtained. Zhai et al. [21] considered the delta winglet vortex generators within a circular tube under Re=5000-25000. Moreover, several attack angles such as 10°, 20°, 30°, and 40° have been tested for vortex generators. The maximum thermal-hydraulic performance of 1.44 was achieved for Re=5000 and an attack angle of 30°. Han et al. [22] investigated the heat transfer characteristics of rectangular vortex generators with a hole for Re=214-10730. It was concluded that despite the fact that the Colburn factor for the vortex generator without a hole was higher than for the one having a hole, when consideringthe thermal-hydraulic performance of the channel, an inverse result was obtained. Aravind and Deepu [23] conducted a research on the convective mass transfer enhancement by lateral sweep vortex generators from the surface of a liquefying substance in turbulent regimes. They observed that the efflux of mass was augmented by increasing the sweep angle of the vortex generator due to the vorticity augmentation. In addition, the characteristics of heat transfer and flow resistance in a rectangular channel with vortex generators under Re=8900-29900 were investigated by Xu et al. [24]. They compared five different vortex generators with the identical frontal area and concluded that in consideration of the thermal-hydraulic performance, the half-cylinder vortex generator was the most suitable. Han et al. [25] applied arc winglet type vortex generators in a fin and tube heat exchanger. In

comparison to the conventional rectangular-winglet vortex generators, 11.5%, 19.9%, and 35.9% enhancements in the Nusselt number were achieved for the equal-perimeter, curved equal-area, and curved equal-perimeter arc vortex generators, respectively. Additionally, Ma et al. [26] examined the longitudinal vortex generators in a thermoelectric power generator. A coupled fluid-thermal-electric model was carried out and 29%-38%, 90%-104%, and 31%-36% enhancements were obtained for the heat input, net power, and thermal conversion efficiency, respectively. Deshmukh et al. [27] used curved delta wing vortex generators to enhance the rate of the heat transfer in tubes under the laminar regime for Re=250-1500. The heat transfer enhancements were obtained between 5 and 15 for the same Reynolds number. The application of longitudinal vortex generators in fin-tube heat exchangers with inline and staggered tube arrangements has been presented by Salviano et al. [28] under Re=250 and 650. They modeled the problem under consideration of a conjugated problem and reported several results. For example, from the heat transfer enhancement point of view, the common-flow-up vortex generator was more appropriate than the common-flow-down vortex generator configuration. Additionally, heat transfer enhancement in the presence of vortex generators for the staggered arrangement was more evident than that of the inline configuration. Moreover, Song et al. [29] examined concave and convex curved vortex generators in the channel of the plate heat exchanger under the laminar regime for Reynolds numbers ranging from 200 to 1400 and attack angles of 20°, 30°, and 40°. It was found that the values of the Nusselt number and goodness factor for the concave curved vortex generator were respectively 19.7% and 11.35% higher than those of the convex vortex generator. Liang et al. [30] applied several arrays of winglet vortex generators in a circular tube for Re=6000-27000 and attack angles of 0°, 10°, 20°, 30°, and 45°. The maximum heat transfer enhancement of 136% was obtained for Re=6000. Thermal enhancement in a solar receiver heat exchanger has been developed by Luo et al. [31]. For this, hey combined various grooves and ribs such as the perturbation triangular ribs, perturbation semi-cylinder ribs, triangular grooves and semi-cylinder grooves with the delta-winglet vortex generator and presented their results for Re=4000-40000. It was concluded that among the cases under consideration, the semi-cylinder grooves in combination with the delta-winglet vortex generator provided the highest thermal performance. Liu et al. [32] published a research work regarding the heat and fluid flow in a circular tube in the presence of rectangular winglet vortex generators for Re=5000-17000. In comparison to the plain tube (without vortex generators), the Nusselt number and friction factor were found to be increased to 1.16-2.49 and 2.09-12.32, respectively.

Examination of the reviewed published works from open literature revealed that there were some restricted studies regarding the heat and fluid flow within the spiral plate heat exchangers despite the various studies available about spiral tube heat exchangers. Moreover, no passive and active heat transfer mechanisms have been developed for spiral plate heat exchangers according to the author's knowledge. On the other hand, it was found that the proposed vortex generators used to enhance the heat transfer in various ducts acted as discontinuous obstacles which were located separately within the ducts. In the present study, a novel and simple approach is suggested to enhance the heat transfer mechanism of the spiral plate heat exchangers. The proposed mechanism was applied to a spiral plate heat exchanger model at which, instead of the conventional discontinuous vortex generators, several rods with the circular cross-section as the continuous vortex generators were inserted within a spiral plate heat exchanger model in the cross-stream plane. It should be mentioned that there have been some restricted works suggesting that continuous vortex generators should be used in order to provide the unsteady flow within the parallel plate heat exchangers [33] and over the hot plate [34]. Several quantitative and qualitative results in terms of the Dean number, non-dimensional diameter of the vortex generators, and the azimuth angle between two neighboring continuous vortex generators have been mentioned in the present study. Computations have been carried out in the laminar regime for a constant Prandtl number of 7.0. Due to the importance of the spiral plate heat exchangers in various industries, this study can be a starting point for further works regarding the spiral plate heat exchangers.

2. Problem description and governing equations

In the present study, heat and fluid flow in a spiral plate heat exchanger model has been investigated two-dimensionally. To enhance the rate of heat transfer, several rods with the circular cross-section as the continuous vortex generators were inserted in the cross-stream plane of the heat exchanger with different azimuth angles such as α=30°, 60°, 90°, and 120° according to the computational domain presented in figure 1.

The azimuth angle is an angle that is measured from the inlet section towards the nearest vortex generator or from each rod towards the next rod. Regarding the two-dimensionality of the problem under consideration, it was assumed that the length of the rods was the same as the heat exchanger length and was sufficiently long in the cross-stream plane. Therefore, the interaction between the working fluid in the spiral plate heat exchanger and these rods formed a two-dimensional flow only in the streamwise and lateral directions. In other words, under the above assumptions, the existence of rods in the cross-stream plane with the same length with the heat exchanger could not deflect the flow in the spanwise direction. Hence, a slice of the heat exchanger was modeled as a two-dimensional problem. Several parameters, in addition to the azimuth angle of vortex generators, such as the Dean number ranging from 500 to 1500 and non-dimensional

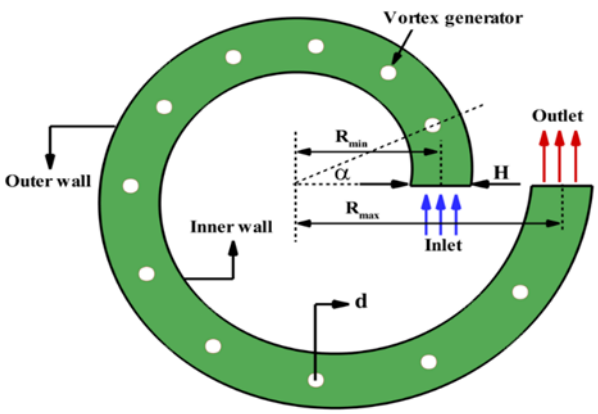

Figure 1. Applied flow domain of a spiral plate heat exchanger model

rod diameters of d/H=0.3, 0.4, and 0.5 were considered. Computations were carried out in laminar regimes for a fluid with Pr=7.0. All heat exchangers under consideration had the same dimensions. For comparison purposes, the conventional plain spiral plate heat exchanger model (without vortex generator) was also computed under corresponding Dean numbers. The time-dependent governing equations for laminar, Newtonian, and two-dimensional flow are as follows;

$$\frac{\partial u}{\partial x}+\frac{\partial v}{\partial y}=0 \tag{1}$$

$$\frac{\partial u}{\partial t}+u\frac{\partial u}{\partial x}+v\frac{\partial u}{\partial y} = -\frac{1}{\rho}\frac{\partial p}{\partial x}+\vartheta\left(\frac{\partial^2 u}{\partial x^2}+\frac{\partial^2 u}{\partial y^2}\right) \tag{2}$$

$$\frac{\partial v}{\partial t}+u\frac{\partial v}{\partial x}+v\frac{\partial v}{\partial y} = -\frac{1}{\rho}\frac{\partial p}{\partial y}+\vartheta\left(\frac{\partial^2 v}{\partial x^2}+\frac{\partial^2 v}{\partial y^2}\right) \tag{3}$$

$$\frac{\partial T}{\partial t}+u\frac{\partial T}{\partial x}+v\frac{\partial T}{\partial y}=\frac{k}{\rho c_p}\left(\frac{\partial^2 T}{\partial x^2}+\frac{\partial^2 T}{\partial y^2}\right) \tag{4}$$

The value of the Dean number was determined as;

$$De=Re\left(\frac{D_h}{R_{ave}}\right)^{0.5} \tag{5}$$

Here, the value of R_{ave} and Re were computed as;

$$R_{ave}=\frac{R_{min}+R_{max}}{2} \tag{6}$$

$$Re=\frac{\rho u_m D_h}{\mu}\,Re=\frac{\rho u_m D_h}{\mu},\qquad D_h=2H \tag{7}$$

To show the temperature field in a non-dimensional form, the following equation was carried out;

$$\theta=\frac{T-T_{in}}{T_w-T_{in}} \tag{8}$$

The value of the mean Nusselt number in each specific time was determined as;

$$Nu=\frac{hD_h}{k} \tag{9}$$

In the above equation;

$$h=\frac{q_w^{"}}{T_w-T_b},\quad q_w^{"}=\frac{q_i^{"}+q_o^{"}}{2} \tag{10}$$

The Time-averaged Nusselt number was calculated using the following equation;

$$Nu=\frac{1}{\Delta t}\int Nu(t)dt \tag{11}$$

in which Δt is a long enough interval time for averaging the flow quantities with respect to the flow time. The value of the non-dimensional pressure drop between the inlet and outlet of the heat exchanger was computed with the following equation;

$$\Delta p^*=\frac{p_{in}-p_{out}}{0.5\rho u_m^2} \tag{12}$$

Values of the root mean square (RMS) of velocity magnitude were computed using the following equation;

$$V_{RMS}=\sqrt{(V-\bar{V})^2} \tag{13}$$

Finally, the thermal-hydraulic performance of the heat exchanger in the presence of continuous vortex generators was obtained using the following equation;

$$PI=\frac{Nu}{Nu_p}\left(\frac{\Delta p^*}{\Delta p_p^*}\right)^{-\frac{1}{3}} \tag{14}$$

In order to solve the governing equations numerically, all derivatives were discretized by means of the finite volume approach. The advection and convective terms were discretized using the second-order upwind scheme while for the discretization of diffusion terms; the central differencing method was applied. On the other hand, a second-order implicit method was carried out to discretize all temporal derivatives in governing equations. To couple the pressure and velocity fields, the **S**emi-Implicit Method for Pressure Linked Equations (SIMPLE) [35] algorithm was implemented. The convergence criteria for all flow variables were set to be less than 10^{-8}. Regarding the applied boundary conditions in the computational domain (figure 1), the uniform velocity and temperature were set at the incoming section and a zero pressure gradient was adopted at the outlet section. Therefore, the velocity and temperature values at the outlet section were determined by extrapolating the corresponding variables. On the other hand, the no-slip velocity condition and a specific temperature were imposed on the inner and outer walls of the heat exchanger. Moreover, similar velocity boundary conditions with heat exchanger walls and zero heat flux were set at boundaries of all vortex generators.

3. Grid size independence study

In the present study, despite the near-wall regions at which the no-slip condition was considered, the non-structured grids were applied according to figure 2. Around the walls, the structured grid distributions with fairly small elements near the inner and outer walls and vortex generators were defined. However, in order to find the optimum grid resolution in each case with respect to computational facilities, a grid test study was performed. As a sample of the grid test, table 1 demonstrates results

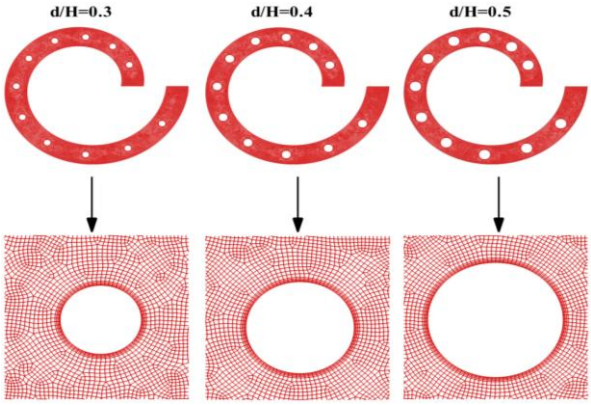

Figure 2: Applied grids in the present study for different d/H values

Table 1. Grid test results for De=1500, d/H=0.4, and α=30°

Grid No.	Node number	Nu	Δp^*
1	14227	79.31	26.32
2	21580	90.04	26.49
3	36573	102.85	26.88
4	54508	104.99	27.09
5	83705	110.76	27.51
6	108446	111.13	27.64

of the grid size independence study for De=1500, d/H=0.4, and α=30°. As seen, six different grid numbers were compared with each other in terms of the time-averaged Nusselt number and non-dimensional pressure drop. Examination of obtained results from grid test revealed that after the fifth grid resolution, further refinement of grids did not alter the obtained thermal-hydraulic results. Therefore, corresponding element sizes were adopted for other cases under consideration. The deviations between "Grid 5" and "Grid 6" were 0.3% and 0.4% for the time-averaged Nusselt number and non-dimensional pressure drop, respectively.

4. Validation of the obtained numerical data

In order to validate the predicted numerical results in the present study, which was a challenge, considering the absence of a similar work, several attempts were made. In the first step, heat and fluid flow between two parallel plates were computed, under velocity and temperature conditions developing simultaneously. The obtained results are shown in figure 3 and compared with available data [36-39] in terms of non-dimensional pressure drop versus the dimensionless axial distance of the hydrodynamic entrance region in addition to the Nusselt number versus the dimensionless axial distances of the thermal entrance region. The comparisons showed excellent agreements between the obtained results and previous data revealing that the applied computer code had sufficient accuracy. In the second step, to be more

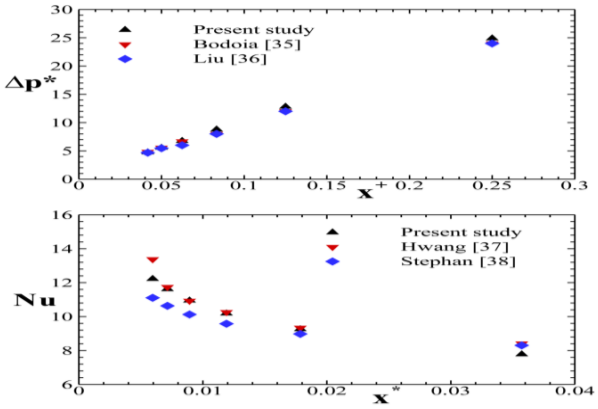

Figure 3: Validation of the applied code against the available data [36-39] for flow between two parallel plates under simultaneously velocity and temperature developing condition; upper image: non-dimensional pressure drop at various dimensionless axial distance of hydrodynamic entrance region and; lower image: Nusselt number at various dimensionless axial distance of thermal entrance region

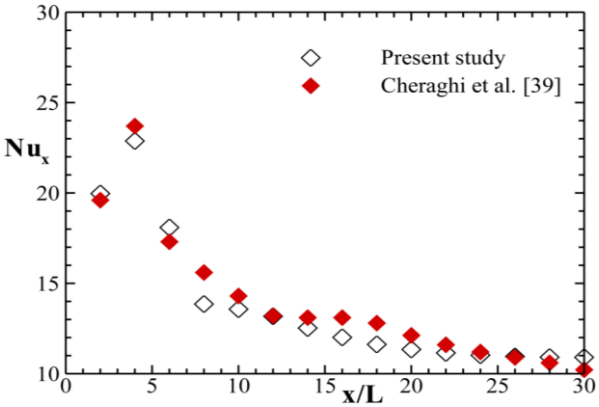

Figure 4: Validation of the applied code against the available data [40] for flow between two parallel plates in the presence of a circular cylinder; distribution of the local Nusselt number with non-dimensional channel length

confident of the obtained results, heat and fluid flow around a circular cross-section rod embedded between two parallel plates were computed and the obtained results for variation of the local Nusselt number with non-dimensional channel length were compared with the published work presented by Cheraghi et al. [40]. Here, "L" is the length of the parallel plates. This comparison is shown in figure 4. Consideration of this comparison confirmed again that the applied computed code had considerable accuracy.

5. Results and discussion

In this section, first of all, the flow physics in the spiral plate heat exchanger model in the presence of circularcontinuous vortex generators has been discussed in detail in terms of variables such as the azimuth angle of vortex generators, non-dimensional diameter of vortex generators, and the Dean number. After that, variations of time-averaged Nusselt number, non-dimensional pressure

drop, and thermal-hydraulic performance of the spiral plate heat exchanger have been illustrated as a function of all variables under consideration.

5.1 Effects of the azimuth angle of continuous vortex generators

In this subsection, effects of the azimuth angle of continuous vortex generators are discussed. Figure 5 illustrates the instantaneous velocity fields in the spiral plate heat exchanger for various azimuth angles such as α=30°, 60°, 90°, and 120° under constant parameters of d/H=0.5 and De=1000. It should be noted that the velocity magnitudes were normalized with respect to the mean velocity within the heat exchanger. Examination of the obtained results showed that the flow within the spiral plate heat exchanger was highly unsteady regardless of the azimuth angle of vortex generators. Development of the unsteady flow in the heat exchanger was due to the vortex shedding process from the sides of the circular cross-section vortex generators. This unsteady flow upgraded the flow mixing within the heat exchanger and therefore, it was expected to enhance the rate of heat transfer within the heat exchanger. Further consideration of velocity fields indicated that the high-velocity pockets downstream of each vertex generator, formed due to the vortex shedding phenomenon, and were strong at α=30°. In addition, by increasing the azimuth angle of continuous vortex generators, these high-velocity pockets attenuated as a function of the azimuth angle. On the other hand, these high-velocity pockets transported high energetic fluid particles from one point to another point and hence, the flow mixing process amplified with growing high velocity pockets. Furthermore, between each neighboring vortex generator, the fluid moved in a wavy passage due to the periodic nature of the vortex shedding process. In high azimuth angles such as α=120°, it seems the shed vortices were eliminated before having an interaction with the next vortex generator. Therefore, in these high azimuth angles, flow immediately upstream of each vortex generator behaved as a steady flow exactly like the conventional spiral plate heat exchanger without continuous vortex generators which was an unwanted situation from the mixing point of view.

In order to reveal the rate of unsteadiness within the spiral plate heat exchanger in the presence of continuous vortex generators, contours of the root mean square of velocity magnitude normalized by mean velocity are presented in figure 6 for various azimuth angles such as α=30°, 60°, 90°, and 120° under constant parameters of d/H=0.5 and De=1000. The higher values of RMS of velocity magnitude demonstrated the higher flow unsteadiness within the heat exchanger. It can be clearly seen that within the spiral plate heat exchanger in general and downstream of each vortex generator in particular, the flow was unsteady. However, it seems that the azimuth angle played a considerable role in development of velocity fluctuations within the heat exchanger. In other words, by increasing the azimuth angle of vortex

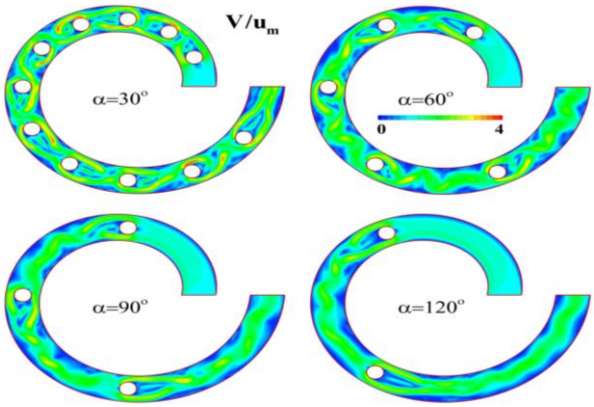

Figure 5. Instantaneous velocity fields of the advanced spiral plate heat exchanger normalized by mean velocity in various azimuth angles under constant parameters of d/H=0.5 and De=1000

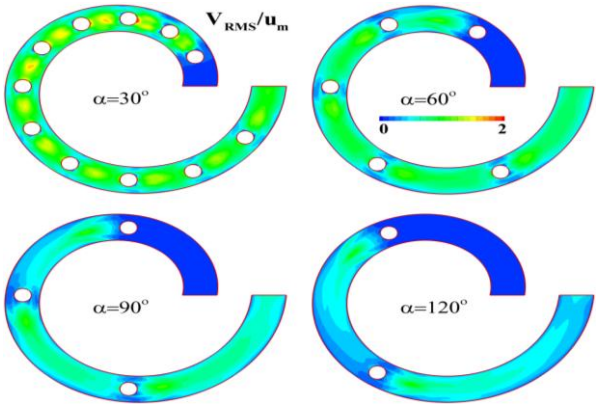

Figure 6. Distributions of the root mean square of velocity magnitude of the advanced spiral plate heat exchanger normalized by mean velocity in various azimuth angles under constant parameters of d/H=0.5 and De=1000

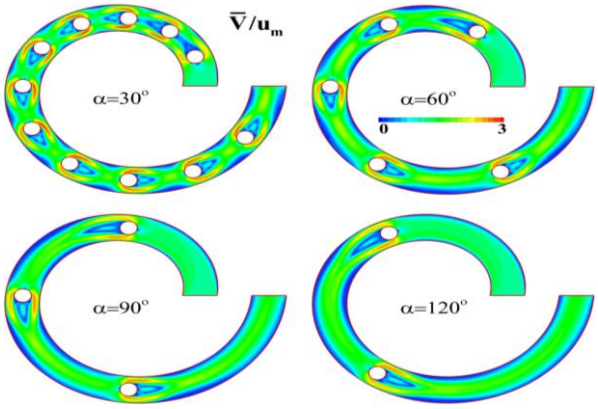

Figure 7. Time-averaged velocity fields of the advanced spiral plate heat exchanger normalized by mean velocity in various azimuth angles under constant parameters of d/H=0.5 and De=1000

generators, the rate of unsteadiness was attenuated strongly so that in the high azimuth angle of α=120°,velocity fluctuations immediately upstream of each vortex generator were minimized as seen in figure 6.

Figure 7 demonstrates time-averaged velocity fields normalized by mean velocity of the heat exchanger for various azimuth angles such as α=30°, 60°, 90°, and 120° under constant parameters of d/H=0.5 and De=1000. Examination of images presented in figure 7 shows that, due to flow blockage between the vortex generators and heat exchanger walls, the flow velocity increased locally at shoulders of all vortex generators in proximity to the heat exchanger walls. This enhancement in the momentum transfer was a positive occurrence from the heat transfer viewpoint since it increased the temperature gradient in near-wall regions. Naturally, an increase in the number of vortex generators augments this positive effect. On the other hand, between two neighboring vortex generators, the velocity gradient in near-wall regions was low. This undesirable situation, which had a negative effect on heat transfer rate between walls and core flow, was more evident on the outer wall of the spiral plate heat exchanger compared with the inner wall mainly due to centrifugal effects in the curved passage. Increasing the azimuth angle reduced the velocity gradient in near-wall regions.

Figure 8 presents time-averaged non-dimensional temperature fields within the spiral plate heat exchanger for various azimuth angles such as α=30°, 60°, 90°, and 120° under constant parameters of d/H=0.5 and De=1000. As expected, due to a high level of unsteadiness within the heat exchanger at α=30°, a considerable temperature penetration can be observed. By increasing the azimuth angle of continuous vortex generators, the core flow experiences low-temperature increments and hence, it can be concluded that the rate of heat transfer reduced as a function of the azimuth angle.

5.2 Effects of the non-dimensional diameter of vortex generators

Another parameter that had a considerable influence on flow nature was the non-dimensional diameter of circular cross-section continuous vortex generators, which is discussed in this subsection. Figure 9 illustrates instantaneous flow patterns for various non-dimensional diameters of vortex generators such as d/H=0.3, 0.4, and 0.5 under constant parameters of α=30° and De=1500. Examination of the instantaneous flow topologies provided extensive information regarding the flow behavior within the spiral plate heat exchanger in the presence of continuous vortex generators.

Several comments can be made regarding the presented results in figure 9. i) the flow streamlines indicated wavy passages for moving flow, demonstrating the highly unsteady flow in the heat exchanger regardless of the d/H value; ii) the shed vortices downstream of each vortex generator showed a tendency to move towards the inner surface due to centrifugal effects of the curved passage; iii)

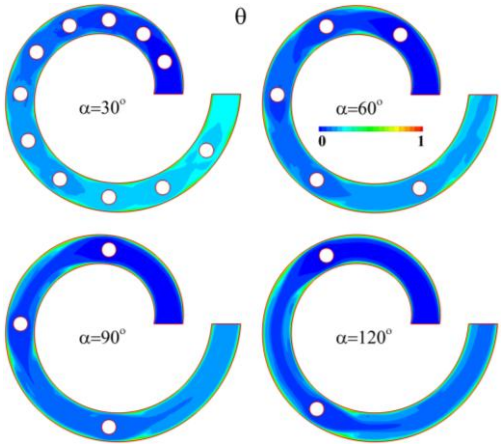

Figure 8. Time-averaged non-dimensional temperature fields of the advanced spiral plate heat exchanger in various azimuth angles under constant parameters of d/H=0.5 and De=1000

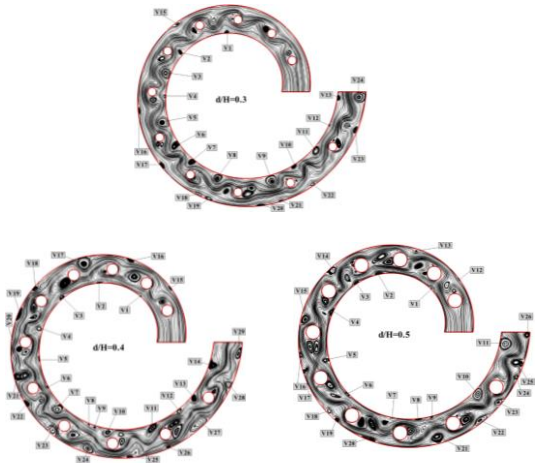

Figure 9. Instantaneous flow topology of the advanced spiral plate heat exchanger in various d/H values under constant parameters of α=30° and De=1500

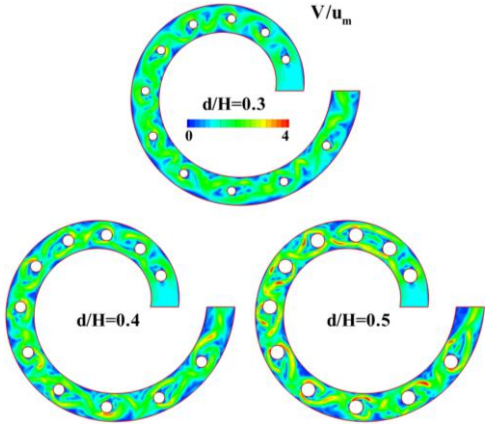

Figure 10. Instantaneous velocity fields of the advanced spiral plate heat exchanger normalized by mean velocity in various d/H values under constant parameters of α=30° and De=1500

the size of the shed vortices from each vortex generator increased by increasing the d/H value; iv) several developing vortices, denoted by V_i (i=1, 2, 3, …), formed on the inner and outer walls of the spiral plate heat exchanger which moved on the walls and had positive effects from the heat transfer perspective. These developing vortices had a completely instantaneous behavior and changed their location rapidly with respect to flow time.

Figure 10 presents instantaneous velocity fields normalized with respect to the mean velocity magnitude within the spiral plate heat exchanger for various non-dimensional diameters of vortex generators such as d/H=0.3, 0.4, and 0.5 under constant parameters of α=30° and De=1500. As seen, in the case of d/H=0.3, the flow nature was completely unsteady and the separated flow from each vortex generator moved periodically towards the walls of the heat exchanger. By increasing the diameter of vortex generators, the high-velocity pockets became more evident. These high-velocity pockets transported high-velocity particles towards the near-wall regions and consequently, the rate of mixing enhanced considerably as seen in the case of d/H=0.5. As a result in this context, it can be reported that the flow mixing was augmented as a function of d/H.

In order to study the rate of unsteadiness and the role of velocity fluctuations within the advanced spiral plate heat exchanger in the presence of continuous vortex generators, distributions of the normalized root mean square of velocity magnitude are shown in figure 11 for various non-dimensional diameters of vortex generators such as d/H=0.3, 0.4, and 0.5 under constant parameters of α=30° and De=1500. Examination of predicted results demonstrates that by increasing the diameter of vortex generators, velocity fluctuations became more evident. These fluctuations were mainly developed in the core flow due to the separation process from vortex generators. In addition, by increasing the d/H value, fluctuations occupied a more significant region within the spiral plate heat exchanger and the unsteady flow showed a tendency to become more dominant in the whole of the channel.

Figure 12 illustrates time-averaged velocity fields normalized with respect to the mean velocity for various non-dimensional diameters of vortex generators such as d/H=0.3, 0.4, and 0.5 under constant parameters of α=30° and De=1500. It is noticed that by increasing the d/H value, the local enhancements of velocity intensified immediately after vortex generators were amplified. This occurrence was due to an increase in the flow blockage level as a function of d/H. On the other hand, due to effects of the centrifugal force, the velocity gradient close to the inner wall was considerably higher than that of the outer wall.

5.3 Effects of the Dean number

The last parameter that is discussed in this subsection

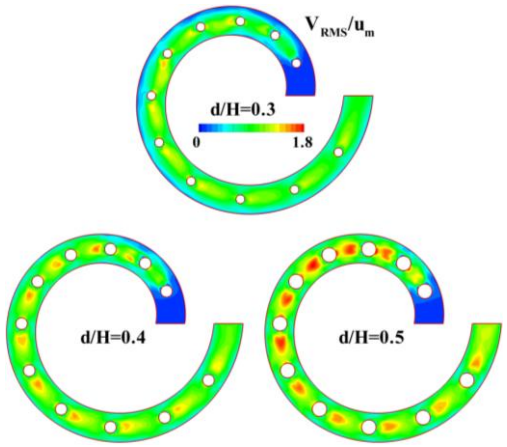

Figure 11. Distributions of the root mean square of velocity magnitude of the advanced spiral plate heat exchanger normalized by mean velocity in various d/H values under constant parameters of α=30° and De=1500

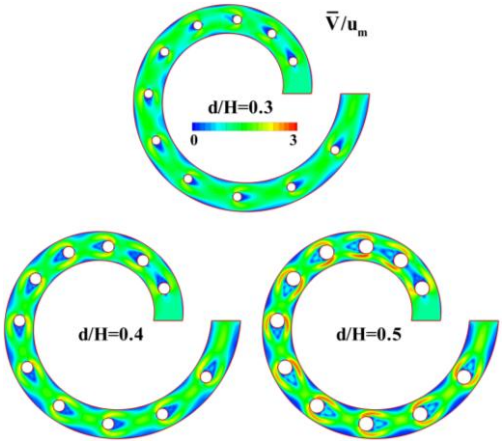

Figure 12. Time-averaged velocity fields of the advanced spiral plate heat exchanger normalized by mean velocity in various d/H values under constant parameters of α=30° and De=1500

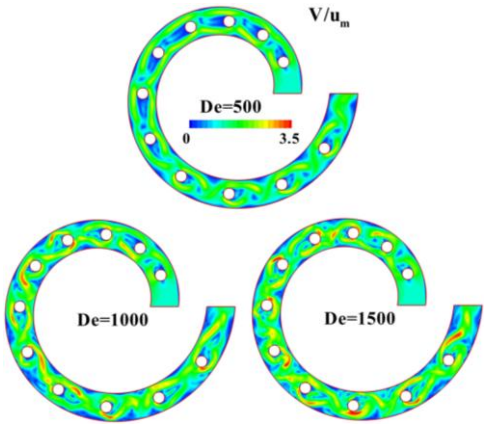

Figure 13. Instantaneous velocity fields of the advanced spiral plate heat exchanger normalized by mean velocity in different Dean numbers under constant parameters of d/H=0.4 and α=30°

is the effects of the Dean number on heat and fluid flow within the spiral plate heat exchanger. As a first qualitative result, distributions of instantaneous velocity fields normalized with respect to the mean velocity are presented in figure 13 for various Dean numbers ranging from 500 to 1500 under constant parameters of d/H=0.4 and α=30°. Examination of instantaneous velocity fields revealed that by increasing the Dean number, high-velocity pockets became more evident and the unsteady flow occupied the whole of the curved channel. These high kinetic energy pockets transported momentum in a wavy passage between vortex generators and hence, the mixing level was augmented as a function of the Dean number.

For enhanced visualization, effects of the Dean number in fields of the root mean square of velocity magnitude normalized by mean velocity are presented in figure 14 for various Dean numbers in the range of 500 to 1500 under constant parameters of d/H=0.4 and α=30°. It can be reported that by increasing the Dean number, velocity fluctuations increased within the spiral plate heat exchanger in general and between two neighboring vortex generators in particular. Therefore, it can be resulted that the Dean number had a positive effect on the level of unsteadiness within the advanced spiral plate heat exchanger.

Figure 15 shows time-averaged velocity fields normalized with respect to mean velocity for various Dean numbers in the range of 500 to 1500 under constant parameters of d/H=0.4 and α=30°. Regarding the Dean number effect on time-averaged velocity distributions within the spiral plate heat exchanger, it can be seen that by increasing the Dean number, recirculating regions downstream of the vortex generators became smaller and hence, the form drag imposed by each continuous vortex generator was attenuated. On the other hand, the core flow velocity between two neighboring vortex generators was enhanced as a function of the Dean number as seen in figure 15.

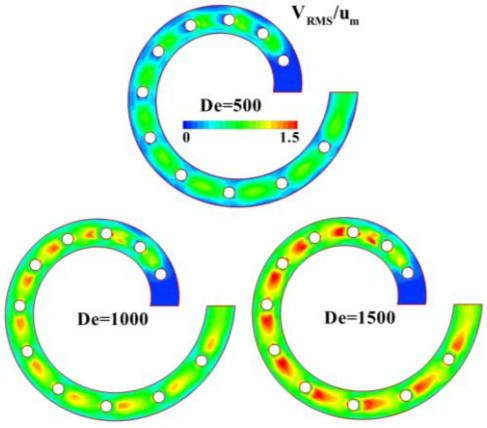

Figure 14. Distributions of the root mean square of velocity magnitude of the advanced spiral plate heat exchanger normalized by mean velocity in different Dean numbers under constant parameters of d/H=0.4 and α=30°

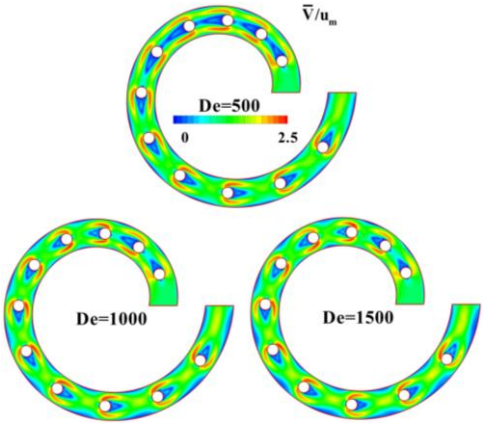

Figure 15. Time-averaged velocity fields of the advanced spiral plate heat exchanger normalized by mean velocity in different Dean numbers under constant parameters of d/H=0.4 and α=30°

5.4 Thermal-hydraulic characteristics

In the last subsection of the obtained results, the quantitative results in terms of the Nusselt number, non-dimensional pressure drop, and thermal-hydraulic performance of the advanced spiral plate heat exchangers are discussed and comparisons with the conventional heat exchanger (without continuous vortex generators) have been presented. As the first result in this context, distributions of the time-averaged Nusselt number versus the azimuth angle of circular cross-section continuous vortex generators are presented in figures 16 (a)-(c) for different d/H and De values. Regarding the obtained results, first of all, a systematic variation of the Nusselt number was observed for each d/H value under a specific Dean number. That is, by increasing the azimuth angle, regardless of the Dean number and d/H value, the rate of the heat transfer in the spiral plate heat exchanger model gradually decreased. This occurrence was mainly due to a reduction in the rate of unsteadiness within the heat exchanger with an increase in the azimuth angle of vortex generators.

On the other hand, regardless of the azimuth angle, under specific Dean numbers, increasing the diameter of vortex generators enhanced the heat transfer rate of the heat exchanger due to development of large vortical structures and high-velocity pockets as a function of d/H. Moreover, as seen, the effects of the d/H in a higher Dean number were more evident compared with the smaller ones. Furthermore, examination of the presented data revealed that the Dean number had a positive effect in augmentation of the heat transfer within the spiral plate heat exchanger for all azimuth angles and d/H values. As a result, all parameters under consideration in the present study such the azimuth angle between the vortex generators, non-dimensional diameter of vortex generators, and the Dean number had effective roles on the heat transfer of a spiral plate heat exchanger. To provide more information regarding the effects of continuous vortex generators in the

Table 2. Heat transfer enhancements of the advanced spiral plate heat exchanger with vortex generators compared with conventional type (without vortex generators) as a function of all under consideration parameters

		Dean number		
		500	1000	1500
α	d/H		Nu/Nu_p	
30°	0.3	2.20	2.65	2.97
	0.4	2.43	2.83	3.64
	0.5	2.72	3.75	4.41
60°	0.3	1.54	1.79	2.20
	0.4	1.85	2.11	2.68
	0.5	2.13	2.77	3.24
90°	0.3	1.29	1.41	1.69
	0.4	1.56	1.67	2.24
	0.5	1.82	2.29	2.70
120°	0.3	1.10	1.11	1.45
	0.4	1.37	1.36	1.99
	0.5	1.65	1.99	2.35

spiral plate heat exchanger, values of heat transfer enhancement with respect to the conventional case (without continuous vortex generators) have been presented in table 2 as a function of the azimuth angle, d/H, and Dean number. As seen, maximum and minimum heat transfer enhancements of 341% and 10% were achieved under α=30°, d/H=0.5, and De=1500 and α=120°, d/H=0.3, and De=500, respectively.

Another important parameter considered in this study, which should be considered by designers, is the variation of the pressure drop within the advanced spiral plate heat exchanger. In this regard, distributions of time-averaged non-dimensional pressure drop versus the azimuth angle between continuous vortex generators are depicted in figures 17 (a)-(c) for different d/H and Dean values. Similar to the variation of the Nusselt number, distributions of non-dimensional pressure drop showed systematic changes with respect to the azimuth angle, d/H, and the Dean number. That is, values of the non-dimensional pressure drop in the spiral heat exchanger were directly proportional directly to d/H and inversely proportional to the Dean number and azimuth angle. However, despite the Nusselt number distributions, effects of d/H on the pressure drop within the heat exchanger were more evident in low Dean numbers. Consideration of values of the pressure drop penalties indicated in table 3 demonstrates that the maximum and minimum pressure drop penalties occurred in α=30°, d/H=0.5, and De=500 and α=120°, d/H=0.3, and De=1500, respectively.

Regarding the simultaneously increase in thermal-hydraulic characteristics, generally, researchers use several criteria to realize the optimum case. One of these parameters is the thermal-hydraulic performance index (PI) which is widely used in previous studies and is presented by Eq. (12). This parameter is based on the concept of "bigger is better" and compares the heat transfer enhancement against the pressure drop penalty, effectively.

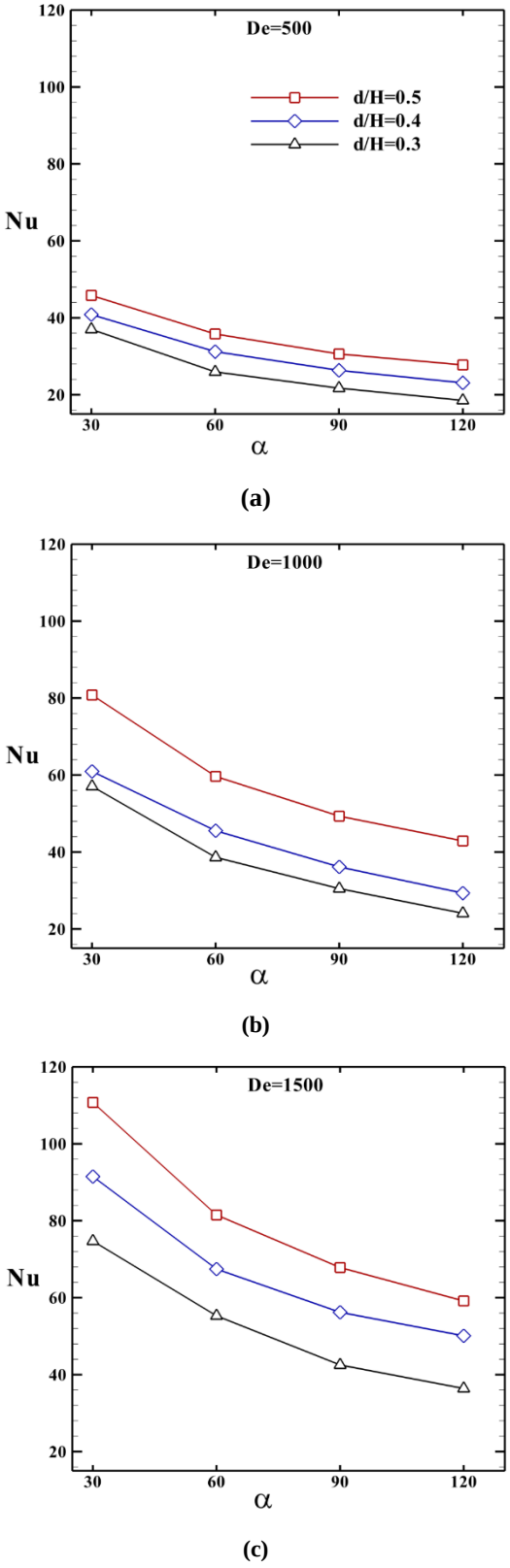

Figure 16. Variations of time-averaged Nusselt number versus the azimuth angle for different d/H values; (a) De=500, (b) De=1000, and (c) De=1500

In accordance with several investigations which have used this criterion to introduce the heat exchanger

Table 3. Values of non-dimensional pressure drop penalty of the advanced spiral plate heat exchanger with vortex generators compared with conventional type (without vortex generators) as a function of all under consideration parameters

		Dean number		
		500	1000	1500
α	d/H	$\Delta p^*/\Delta p^*_p$		
30°	0.3	13.10	8.35	6.86
	0.4	18.44	12.09	10.06
	0.5	29.10	17.83	14.79
60°	0.3	6.22	4.03	4.07
	0.4	9.50	6.13	5.11
	0.5	15.34	8.76	7.13
90°	0.3	5.64	3.36	2.75
	0.4	7.38	4.28	3.54
	0.5	10.36	6.48	5.10
120°	0.3	4.66	2.74	2.26
	0.4	5.80	3.40	2.85
	0.5	7.89	4.22	3.74

performance, here, variations of this parameter are illustrated in figures 18 (a)-(c) against the azimuth angle for different Dean numbers and d/H values. In the case with d/H=0.3 in which effects of the azimuth angle was more evident in comparison to the other d/H values, the spiral plate heat exchanger performance increased with a decrease in the azimuth angle between the continuous vortex generators and an increase in the Dean number. The maximum thermal-hydraulic performance of the spiral plate heat exchanger in the case of d/H=0.3 occurred for α=30° and De=1500 up to 1.57 as seen in figure 18 (a). By increasing the diameter of the continuous vortex generators, the difference between values of performance indices in all Dean numbers decreased as presented in figures 18 (b) and (c). In the case of d/H=0.4, the maximum performance of the advanced spiral plate heat exchanger developed for α=30° and De=1500 as 1.70. This enhancement in the thermal-hydraulic performance reached to 1.81 in d/H=0.5 for α=30° and De=1500. Table 4 separates effective cases (PI>1) from ineffective ones (PI<1) to provide a guideline for thermal designers. It should be noted that in the effective cases, the heat transfer enhancement overcame the pressure drop penalty and in the ineffective cases this did not happen.

6. Conclusions

In the present numerical study, circular cross-section continuous rods as an innovative and simple type of vortex generators were introduced and applied for a spiral plate heat exchanger model. All effective parameters on the heat and fluid flow within the advanced spiral plate heat exchanger such as the azimuth angle between vortex generators variations from 30° to 120°, non-dimensional diameters of vortex generators of d/H=0.3, 0.4, and 0.5, and the Dean number in the range of 500-1500 have been discussed in detail. Computations were performed for a constant Prandtl number of 7.0 under the laminar regime.

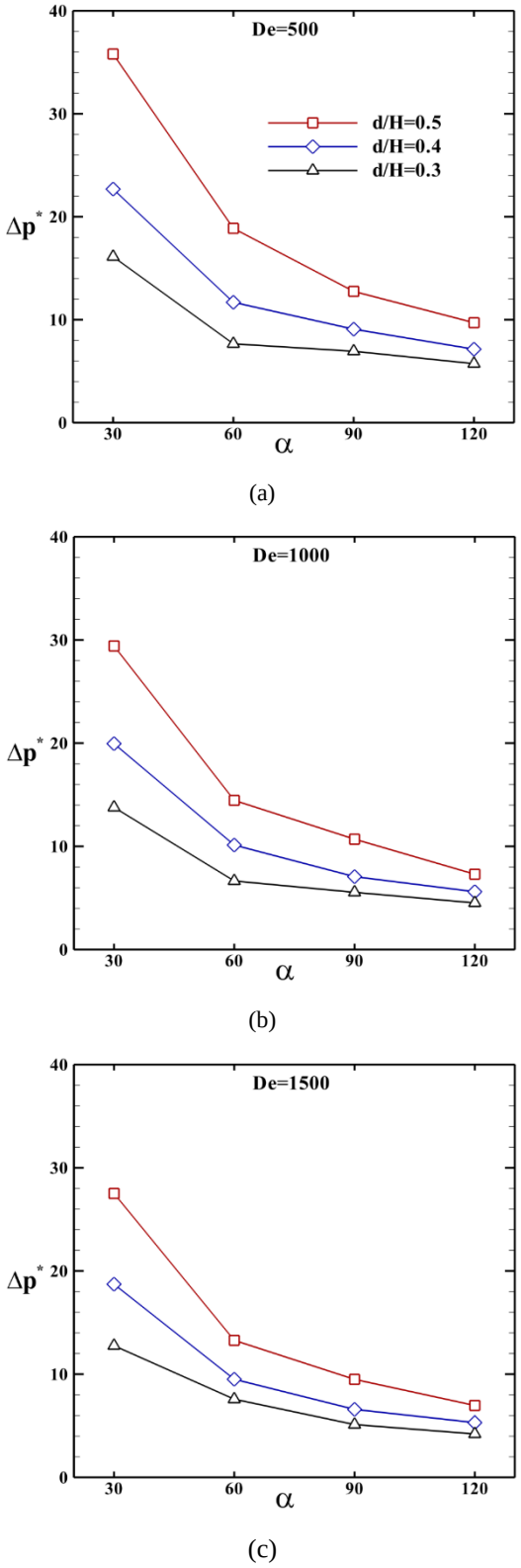

Figure 17. Variations of time-averaged non-dimensional pressure drop versus the azimuth angle for different d/H values; (a) De=500, (b) De=1000, and (c) De=1500

The applied computer code was validated against the several available data and obtained good agreements with comparisons. Several qualitative and quantitative results were presented in this investigation. It was found that the

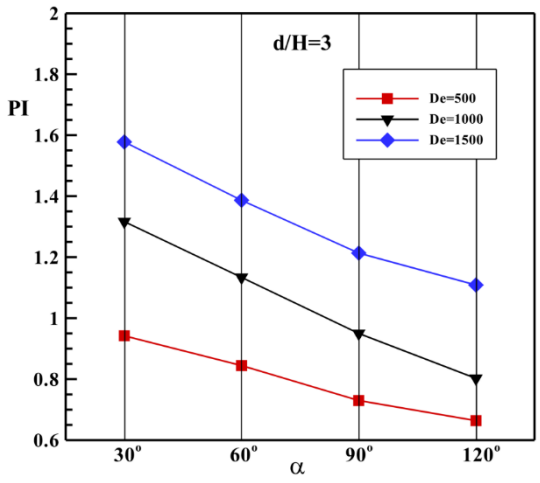

(a)

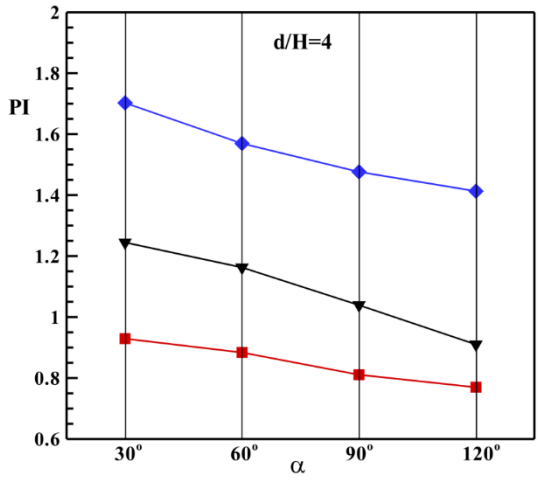

(b)

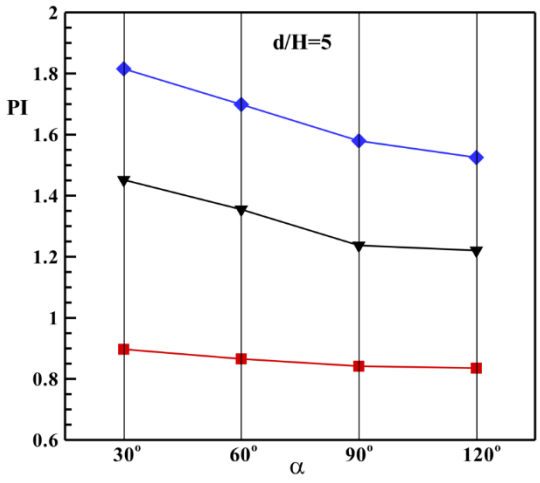

(c)

Figure 18. Variations of thermal-hydraulic performance index versus the azimuth angle for different Dean numbers; (a) d/H=0.3, (b) d/H=0.4, and (c) d/H=0.5

flow behavior in a spiral plate heat exchanger changed considerably with the azimuth angle, diameter of vortex generators, and the Dean number. That is, the rate of unsteadiness increased with increasing the d/H value and

Table 4. Separating the effective cases (E) with PI>1 from ineffective cases (IE) with PI<1

		Dean number		
		500	1000	1500
α	d/H	Effective (E) and ineffective (IE) cases		
30°	0.3	IE	E	E
	0.4	IE	E	E
	0.5	IE	E	E
60°	0.3	IE	E	E
	0.4	IE	E	E
	0.5	IE	E	E
90°	0.3	IE	IE	E
	0.4	IE	E	E
	0.5	IE	E	E
120°	0.3	IE	IE	E
	0.4	IE	IE	E
	0.5	IE	E	E

the Dean number and with decreasing the azimuth angle of vortex generators. On the other hand, the systematic variations in the heat transfer rate were observed as a function of d/H, De, and the number of vortex generators. The maximum heat transfer enhancement of 341% was successfully achieved at α=30°, d/H=0.5, and De=1500. Finally, the maximum thermal-hydraulic performance of 1.81 was established at α=30°, d/H=0.5, and De=1500.

Nomenclature

c_p	Specific heat (J/kg.°C)
d	Diameter of vortex generators (m)
D_h	Hydraulic diameter of the flow passage (m)
De	Dean number
h	Convective heat Transfer coefficient (W/m².°C)
H	Distance between inner and outer walls (m)
L	Channel length (applied only in validation study) (m)
k	Conductivity (W/m.°C)
p	Pressure (Pa)
PI	Thermal-hydraulic performance index
Δp^*	Non-dimensional pressure drop
q''	Heat flux (W/m²)
Nu_x	Local Nusselt number
Nu	Time-averaged Nusselt number
R_{ave}	Average radius of the spiral plate heat exchanger model (m)
Re	Reynolds number
t	Time (s)
Δt	Time interval for time-averaging the flow quantities (sec)
T	Temperature (°C)
u	Streamwise velocity (m/s)

u_m	Mean velocity in each section of the curved channel (m/s)
v	Lateral velocity (m/s)
V	Instantaneous velocity magnitude (m/s)
V_{RMS}	Root mean square of velocity magnitude (m/s)
$\overline{V}$	Time-averaged velocity magnitude (m/s)
x	Horizontal coordinate (m)
x^+	Dimensionless axial distance of the hydrodynamic entrance region
x^*	Dimensionless axial distances of the thermal entrance region
y	Lateral coordinate (m)

Greek symbols

ρ	Density (kg/m^3)
μ	Dynamic viscosity (kg/m.s)
ϑ	Kinematic viscosity (m^2/s)
θ	Non-dimensional temperature
α	Azimuth angle between the vortex generators (˚)

Subscripts

b	Bulk
i	Inner wall
in	Inlet
o	Outer wall
p	Plain case (without vortex generator)
w	Wall

References

[1] Saeidi, R., Noorollahi, Y. and Esfahanian, V., 2018. Numerical simulation of a novel spiral type ground heat exchanger for enhancing heat transfer performance of geothermal heat pump, Energy Conversion and Management ,168 ,pp.296-307.

[2] Bahiraei, M. and Ahmadi, A.A., 2018. Thermohydraulic performance analysis of a spiral heat exchanger operated with water – alumina nanofluid : Effects of geometry and adding nanoparticles. Energy Conversion and Management, 170, pp.62-72.

[3] Zhao, Q., Liu, F., Liu, C., Tian, M. and Chen, B., 2017. Influence of spiral pitch on the thermal behaviors of energy piles with spiral-tube heat exchanger. Applied Thermal Engineering, 125, pp.1280-1290.

[4] Li, H., Nagano, K. and Lai, Y., 2012. Heat transfer of a horizontal spiral heat exchanger under groundwater advection. International Journal of Heat and Mass Transfer, 55, pp.6819–6831.

[5] Dehghan B, B., 2017. Experimental and computational investigation of the spiral ground heat exchangers for ground source heat pump applications Coefficient of Performance. Applied Thermal Engineering, 121, pp.908–921.

[6] Wang, S., Jian, G., Xiao, J., Wen, J., Zhang, A. and Tu, J., 2018. Fluid-thermal-structural analysis and structural optimization of spiral- wound heat exchanger. International Communication in Heat and Mass Transfer, 95, pp.42–52.

[7] Abdel-Aziz, M.H. and Sedahmed, G.H., 2019. Natural convection mass and heat transfer at a horizontal spiral tube heat exchanger. Chemical Engineering Research and Design, 145, pp.122-127.

[8] Sharqawy, M.H., Saad S.M.I. and Ahmed, K.K., 2019. Effect of flow configuration on the performance of spiral- wound heat exchanger. Applied Thermal Engineering, 161, 114157.

[9] Ardahaie, S.S., Hosseini, M.J., Ranjbar, A.A. and Rahimi, M., 2019. Energy storage in latent heat storage of a solar thermal system using a novel flat spiral tube heat exchange. Applied Thermal Engineering, 159, 113900.

[10] Mohamad Gholy Nejad, P., Solaimany Nazar, A.R., Rahimi-Ahar, Z. and Rajati, H., 2019. Investigation on turbulent nanofluid flow in helical tube in tube heat exchangers. Journal of Heat and Mass Transfer Research, 6, pp.31-39.

[11] da Silva, F.A.S., Dezan, D.J., Pantaleão, A.V. and Salviano, L.O., 2019. Longitudinal vortex generator applied to heat transfer enhancement of a flat plate solar water heater. Applied Thermal Engineering, 158, 113790.

[12] Wang, Y., Liu, P., Shan, F., Liu, Z. and Liu, W., 2018. Effect of longitudinal vortex generator on the heat transfer enhancement of a circular tube. Applied Thermal Engineering, 148, pp.1018-1028.

[13] Garelli, L., Rodriguez, G.R., Dorella, J.J. and Storti, M.A., 2019. Heat transfer enhancement in panel type radiators using delta-wing vortex generators. International Journal of Thermal Science, 137, pp.64–74.

[14] Yang, J.S., Jeong, M., Park, Y.G. and Ha, M.Y., 2019. Numerical study on the flow and heat transfer characteristics in a dimple cooling channel with a wedge-shaped vortex generator. International Journal of Heat and Mass Transfer, 136, pp.1064–1078.

[15] Ke, Z., Chen, C.L., Li, K., Wang, S. and Chen, C.H., 2019. Vortex dynamics and heat transfer of longitudinal vortex generators in a rectangular channel. International Journal of Heat and Mass Transfer, 132, pp.871–885.

[16] Jiansheng, W., Yu, J. and Xueling, L., 2019. Heat transfer and flow characteristics in a rectangular channel with small scale vortex generators. International Journal of Heat and Mass Transfer, 138, pp.208–225.

[17] Oneissi, M., Habchi, C., Russeil, S., Lemenand, T. and Bougeard, D., 2018. Heat transfer enhancement of inclined projected winglet pair vortex generators with protrusions. International Journal of Thermal Science, 134, 541–551.

[18] Samadifar, M. and Toghraie, D., 2018. Numerical simulation of heat transfer enhancement in a plate-fin heat exchanger using a new type of vortex generators. Applied Thermal Engineering, 133, pp.671-681.

[19] Gallegos, R.K.B. and Sharma, R.N., 2019. Heat transfer performance of flag vortex generators in rectangular channels. International Journal of Thermal Science, 137, pp.26–44.

[20] Li, J., Dang, C. and Hihara, E., 2019. Heat transfer enhancement in a parallel, finless heat exchanger using a longitudinal vortex generator, Part A : Numerical investigation. International Journal of Heat and Mass Transfer, 128, pp.87–97.

[21] Zhai, C., Islam, M.D., Simmons, R. and Barsoum, I., 2019. Heat transfer augmentation in a circular tube with delta winglet vortex generator pairs. International Journal of Thermal Science, 140, pp.480–490.

[22] Han, Z., Xu, Z. and Wang, J., 2018. Numerical simulation on heat transfer characteristics of rectangular vortex generators with a hole. International Journal of Heat and Mass Transfer, 126, pp.993–1001.

[23] Aravind G.P. and Deepu, M., 2017. Numerical study on convective mass transfer enhancement by lateral sweep vortex generators. International Journal of Heat and Mass Transfer, 115, pp.809–825.

[24] Xu, Z., Han, Z., Wang, J. and Liu, Z., 2018. The characteristics of heat transfer and flow resistance in a rectangular channel with vortex generators. International Journal of Heat and Mass Transfer, 116, pp.61–72.

[25] Han, H., Wang, S., Sun, L., Li, Y. and Wang, S., 2019. Numerical study of thermal and flow characteristics for a fin-and-tube heat exchanger with arc winglet type vortex generators. International Journal of Refrigeration, 98, pp.61-69.

[26] Ma, T., Pandit, J., Ekkad, S.V., Huxtable, S.T. and Wang, Q., 2015. Simulation of thermoelectric-hydraulic performance of a thermoelectric power generator with longitudinal vortex generators. Energy, 84, pp.695-703.

[27] Deshmukh, P.W., Prabhu, S.V. and Vedula, R.P., 2016. Heat transfer enhancement for laminar flow in tubes using curved delta wing vortex generator inserts. Applied Thermal Engineering, 106, 1415–1426.

[28] Salviano, L.O., Dezan, D.J. and Yanagihara, J.I., 2016. Thermal-hydraulic performance optimization of inline and staggered fin-tube compact heat exchangers applying longitudinal vortex generators. Applied Thermal Engineering, 95, pp.311–329.

[29] Song, K., Tagawa, T., Chen, Z. and Zhang, Q., 2019. Heat transfer characteristics of concave and convex curved vortex generators in the channel of plate heat exchanger under laminar flow. International Journal of Thermal Science, 137, pp.215–228.

[30] Liang, G., Islam, M.D., Kharoua, N. and Simmons, R., 2018. Numerical study of heat transfer and flow behavior in a circular tube fitted with varying arrays of winglet vortex generators. International Journal of Thermal Science, 134, pp.54–65.

[31] Luo, L., Wen, F., Wang, L., Sundén, B. and Wang, S., 2016. Thermal enhancement by using grooves and ribs combined with delta-winglet vortex generator in a solar receiver heat exchanger. Applied Energy, 183, pp.1317–1332.

[32] Liu, H.L., Li, H., He, Y.L. and Chen, Z.T., 2018. Heat transfer and flow characteristics in a circular tube fitted with rectangular winglet vortex generators. International Journal of Heat and Mass Transfer, 126, pp.989–1006.

[33] Hassanzadeh, R. and Tokgoz, N., 2019. Analysis of heat and fluid flow between parallel plates by inserting triangular cross-section rods in the cross-stream plane. Applied Thermal Engineering, 160, 113981.

[34] Hassanzadeh, R., 2018. Effects of Unsteady flow generation over a hot plate on the cooling mechanism using a rotating cylinder. Arabian Journal for Science and Engineering, 43, pp.4463-4473.

[35] Patankar, S.V., 1980. Numerical heat transfer and fluid flow. Taylor & Francis, New York.

[36] Bodoia, J.R., 1959. The finite difference analysis of confined viscous flows. Ph.D. Thesis. Carnegie Institute of Technology, Pittsburgh, Pennsylvania.

[37] Liu, J., 1974. Flow of a Bingham fluid in the entrance region of an annular tube. M.S. Thesis. University of Wisconsin-Milwaukee.

[38] Hwang, C.L., 1973. Personal communication. Dep. Ind. Eng., Kansas State University, Manhattan.

[39] K. Stephan, K., 1959. Wärmeübergang und druckabfall bei nicht ausgebildeterlaminar strömung in rohren und in ebenen spalten. Chemie Ingenieur Technik, 31, pp.773-778.

[40] Cheraghi, M., Raisee, M. and Moghaddami, M., 2014. Effect of cylinder proximity to the wall on channel flow heat transfer enhancement. Comptes Rendus Mécanique, 342, pp.63–72.